SIMULATION OF MICROWAVE BACKSCATTERING FROM SEA SURFACE USING AN IMPROVED TWO-SCALE MODEL

Honglei Zheng [1]*, Jie Zhang* [1]*, Ali Khenchaf* [2]*, Yanmin Zhang* [3]*, Yunhua Wang* [3]

[1] College of Oceanography and Space Informatics, China University of Petroleum (East China), Qingdao 266580, China
[2] Lab-STICC, UMR CNRS 6285, ENSTA Bretagne, Brest 29806, France
[3] College of Information Science and Engineering, Ocean University of China, Qingdao 266100, China
Email: *hongleizheng@hotmail.com*

ABSTRACT

The two-scale model (TSM) has been frequently used in the study of EM (electromagnetic) scattering from rough surface due to its simple and practical merit. However, for microwave scattering from sea surface, it cannot provide accurate predictions for *hh* (horizontal) polarization. To overcome this problem, an improved version of the TSM (ITSM) which can be better used for predicting microwave scattering from sea surface is proposed in this paper. In the ITSM, we propose to use two cutoff parameters to separate sea surface roughness. For $k_w<k_{cs}$, the KA-SP (Kirchhoff approximation-stationary phase approximation) rather than KA-GO (Kirchhoff approximation-geometric optics approximation) is employed to simulate the specular scattering component. For $k_w>k_{cb}$, the SPM modulated by tilts of large-scale waves is employed to simulate the Bragg scattering component. The values of k_{cs} and k_{cb} are chosen according to the validity conditions of the KA and the SPM. The numerical comparisons illustrate that the ITSM performs better than the TSM and the SSA-1, especially in the prediction of *hh* polarized scattering coefficient.

Index Terms— Microwave backscattering, Two-scale model, Kirchhoff approximation, Ocean remote sensing

1. INTRODUCTION

Spaceborne and airborne microwave radars provide valuable observations in ocean remote sensing and it plays an increasingly important role in the detection and monitoring of targets in the ocean environment. In the past decades, numerous airborne and space-born radars operate at various band have been developed for ocean observation, e.g. the C band Advanced Synthetic Aperture Radar (ASAR) on the European Space Agency (ESA)'s ENVISAT-1 satellite; the full polarimetric SAR on the Canadian Space Agency's Radarsat-2, etc. The basic principle of a radar to observe sea phenomena is that it transmits EM waves with a certain frequency towards sea surface, and part of scattered EM waves will be received again by radar after interacting with sea waves. The scattering coefficient (σ_0 or NRCS, normalized radar cross section) which can be derived from the echoes are sensitive to the ocean-surface roughness due to gravity-capillary surface waves.

Establishing an accurate model to describe the relationship between the scattering coefficient and physical parameters (e.g. wind speed, sea surface temperature, etc.) is of critical important for ocean observation [1]. In practical applications, geophysical model functions (GMFs) are often used to model the responses of incidence angle, wind speed and wind direction on the scattering coefficient [2]. However, like all other empirical models, GMFs have limited physical meanings which make it difficult for more physical interpretations. Unlike the empirical models, approximate methods are rigorously derived under certain assumptions and have been proven to be effective methods under certain conditions. Among the approximate methods, the KA and the SPM are of most significant. The combination of these two methods, named the two-scale model, has been well used to study the EM scattering from rough sea surface and the theoretical and experimental results appear to be in good agreement. However, it is recognized that, it is difficult to obtain a reasonable prediction of the scattering coefficient over a large range of radar frequencies, incidence angles, for the different polarization states and various conditions of wind and waves using the classic TSM. In particular, it has been mentioned in many publications, the TSM may provide consistent results for *vv* polarization, are not in agreement with observations for *hh* polarization.

In this paper, an improved TSM which has been proven more accurate for *hh* polarized scattering coefficient prediction is proposed in this work. The present paper is organized as follows: in section 2, the validity conditions of the KA and SPM are reviewed briefly, and the improved TSM is introduced. Some meaningful simulated results are presented and discussed in section 3. The conclusions are drawn in the final section.

2. THE IMPROVED TWO-SCALE MODEL

2.1. The specular scattering component

In the TSM, the Kirchhoff approximation (or the tangent plane approximation) is often used to simulate the EM scattering from large scale roughness surface. According to the Kirchhoff approximation, the scattered field at any point within a source-free region bounded by a closed surface can be expressed in terms of the tangential fields on the surface. The validity conditions for KA are [1]

$$k_i l > 6 \tag{1}$$

$$R_c > \lambda_i \tag{2}$$

where k_i is the incidence wave number, λ_i is the incidence wave length, l is correlation length and R_c is the radius of curvature.

Considering the C band SAR has been widely used in ocean observation, e.g. Radarsat-2, ENVSAT ASAR, etc. Hereafter, C band (the frequency of incident wave is 5.3 GHz) is used here as a case study to perform detailed simulations and discussion. For C band, the validity condition of Eq.(1) can be rewritten as

$$l > \frac{6}{k_i} \approx 0.054 \tag{3}$$

The correlation length of sea surface can be approximately calculated using

$$l = 0.154 \times U_{10}^{2.04} \text{ with } U_{10} \in [2;17]\,m/s \tag{4}$$

where U_{10} denotes the wind speeds at 10 m height above sea surface. It can be easily known that the validity condition is satisfied for C band.

The RMS (root mean square) radius of curvature of large-scale wave sea surface can be calculated with the sea spectrum, i.e.

$$R_c = \frac{1}{\sqrt{\int_0^{k_c} k_w^4 S(k_w)\,dk_w}} \tag{5}$$

where k_w is the spatial wavenumber of sea waves. $S(k_w)$ denotes the sea spectrum. In this paper, the spectrum proposed by Elfouhaily et al. is employed [3]. To satisfy Eq.(2), the RMS radius of curvature of the surface should be larger than the incidence wavelength. The cutoff wavenumber for specular scattering component (k_{cs}) is empirically set to be 188 rad/m for U_{10}<20m/s.

After applying the tangent plane approximation, it is still impossible to obtain an analytical solution. Stationary phase approximation is used to simplify the scattered field expression. With the tangent plane approximation and the stationary phase approximation, the scattering coefficient in bistatic configuration can be expressed as

$$\sigma_{0\alpha\alpha_0} = \frac{\left|k_i U_{\alpha\alpha_0}\right|^2}{4\pi A_0} \left\langle |I|^2 \right\rangle \tag{6}$$

where $\alpha\alpha_0 \in \{hh, hv, vh, vv\}$, h denotes horizontal polarization and v denotes vertical polarization, respectively. A_0 is the illuminated area. $U_{\alpha\alpha_0}$ are polarization-dependent coefficients. In the derivation of σ_0 , the main task is to calculate the $\left\langle |I|^2 \right\rangle$. The $\left\langle |I|^2 \right\rangle$ can be expressed as

$$\left\langle |I|^2 \right\rangle = \int\int \left\langle \exp\left[jk_i (\hat{\mathbf{n}}_s - \hat{\mathbf{n}}_i) \cdot (\mathbf{r}' - \mathbf{r}'') \right] \right\rangle dS' dS'' \tag{7}$$

where $\hat{\mathbf{n}}_i$ is unit vector in the direction of incidence, $\hat{\mathbf{n}}_s$ is the unit vector in scattering direction. When the surface height is normally distributed, it can be written as:

$$\begin{aligned} \left\langle |I_1|^2 \right\rangle \quad & \frac{q^2}{|q_z|^2} (2L)^2 \int_{-2L}^{L} \int_{-2L}^{2L} \exp\left[jq_x u + jq_y v \right] \\ & \cdot \exp \quad -q_z^2 \delta^2 (1-\rho) \big] dudv \end{aligned} \tag{8}$$

In Eq.(8), $2L$ is the illuminated length, and

$$\begin{cases} q_x = k_i (\sin\theta_s \cos\varphi_s \quad \sin\theta_i \cos\varphi_i) \\ q_y = k_i (\sin\theta_s \sin\varphi_s \quad \sin\theta_i \sin\varphi_i) \\ q_z = k_i (\cos\theta_s \quad \cos\theta_i) \\ q^2 = q_x^2 + q_y^2 + q_z^2 \end{cases} \tag{9}$$

where θ_i is the incidence angle, θ_s is the scattering angle, φ_i is the incidence azimuth angle, and φ_s is the scattering azimuth angle. δ and ρ are the RMS height and the autocorrelation coefficient, respectively.

It is customary to reduce Eq.(8) to a single integral using Bessel transforms. The scattering coefficient can be finally expressed as

$$\begin{aligned} \sigma_{0,\alpha\alpha_0}^{KA-SP} = & \frac{q^2 \left|k_i R_{\alpha\alpha_0}\right|^2}{q_z^2} \exp\left[-q_z^2 \delta^2\right] \cdot \int_0^r \exp\left(q^2 W_0\right) \\ & \cdot \sum_m J_{-2m}(r q_{xy}) I_m\left(q_z^2 W\right) \exp[2jm\chi] r dr \end{aligned} \tag{10}$$

where $q_{xy} = \sqrt{q_x^2 + q_y^2}, \chi = \arctan\left(\frac{q_y}{q_x}\right)$. In Eq.(10),

$$\begin{aligned} W(\mathbf{r}) &= W(r,\phi) = W_0(r) - \cos(2\phi) W_2(r) \\ W_0(r) &= \int_0^{k_c} S_0(k_w) J_0(k_w r)\, dk_w \\ W_2(r) &= \int_0^{k_c} S_0(k_w) J_2(k_w r) \Delta(k_w)\, dk_w \end{aligned} \tag{11}$$

where $S_0(k_w)$ denotes the omnidirectional part of sea spectrum, k_w is the wavenumber of sea wave. $J_m(\cdot)$ is the Bessel function of the first kind and of order m. Note that only the tangent plane approximation and stationary phase approximation have been involved in the derivation of the scattering coefficient expressed in Eq.(10). The KA-SP reduces to the KA-GO which is commonly used in TSM under the condition that $\left(q_z\delta\right)^2$ is large enough. Fig. 1 shows the comparisons between the KA-SP and the KA-GO. As shown in Fig. 1, the differences between the scattering coefficient estimated using KA-SP and KA-GO are not significant for incidence angle about smaller than 25°. While the scattering coefficient of KA-GO is remarkably underestimated than that of KA-SP for an incidence angle larger than 25°.

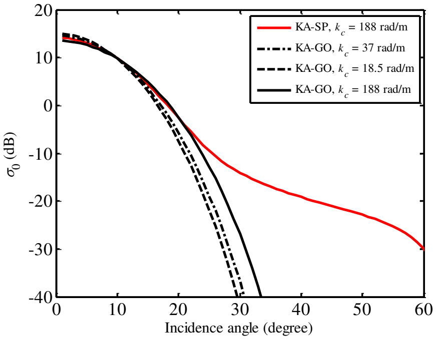

Fig. 1 Comparison of the scattering coefficient between the KA-SP and the KA-GO, f = 5.3GHz, U_{10}=7m/s, upwind.

2.2. The Bragg scattering component

The SPM is used to simulate the EM scattering from small scale waves of sea surface. The validity conditions of SPM are

$$k_i\delta < 0.3 \tag{12}$$

$$z_s < 0.3 \tag{13}$$

where z_s denotes the RMS slope. The RMS height and RMS slope of sea surface can be estimated using

$$\delta = \sqrt{\int_{k_c}^{\infty} S\left(k_w\right) dk_w} \tag{14}$$

$$z_s = \sqrt{\int_{k_c}^{\infty} k_w^2 S\left(k_w\right) dk_w} \tag{15}$$

Similar, the cutoff wavenumber for Bragg scattering component (k_{cb}) can be found through Eq.(12)~Eq.(15) which is set as 27 rad/m in case of U_{10}<20m/s.

2.3. The improved two-scale model

To take the contribution induced by specular scattering at moderate incidence angles, the scattering coefficient related to specular scattering can be calculated using KA-SP rather than KA-GO. Accordingly, the improved two-scale model is finally expressed as

$$\sigma_{pq}^{ITSM} = \sigma_{\alpha\alpha}^{KA-SP} + \int_{-\infty}^{\infty}\int_{-\cot\theta_i}^{\infty} \sigma_{\alpha\alpha_0}^{SPM} P_{\theta_i}\left(z_x, z_y\right) dz_x dz_y \tag{16}$$

where $P_{\theta_i}\left(z_x, \ _y\right)$ is the slope probability density function as viewed from the incidence direction. In the following simulation, the sea surface slopes are assumed Gaussian distributed.

3. NUMERICAL SIMULATION AND DISCUSSIONS

In this part, the scattering coefficients estimated using the proposed ITSM are compared with those obtained using the traditional TSM, the first order small slope approximation (SSA-1) [4] and the geophysical model function (GMF). Notably, GMFs are derived based on a large number of measurements. It has been proven that GMFs could provide accurate predictions in practical applications. Thus, the scattering coefficient estimated using GMFs can be regarded as reliable references. In the following, the scattering coefficient predicted using the C band GMF CMOD5n [2] is served as references and a polarization ratio (*PR*) model [5] is employed to convert the scattering coefficient from the *vv* polarization to the *hh* polarization.

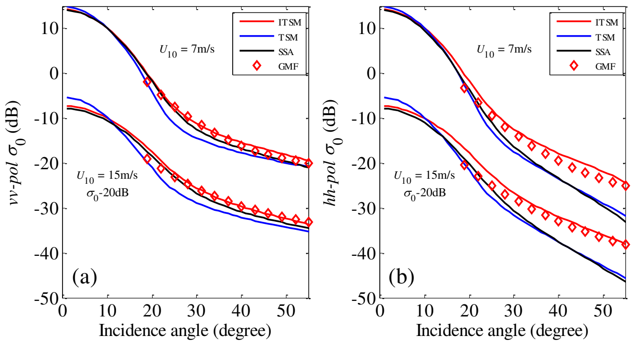

Fig. 2 The simulated results using the ITSM, the TSM and the SSA-1 are compared with those obtained using the GMF with respect to incidence angle, upwind. Note that the curves for $\sigma_0 - 20dB$ are plotted for the cases of U_{10}=15m/s. (a) *vv* polarization (b) *hh* polarization.

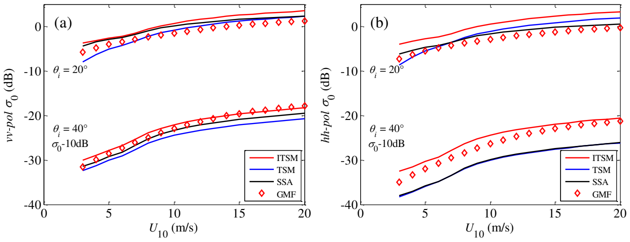

Fig. 3 The simulated results using the ITSM, the TSM and the SSA-1 are compared with those obtained using the GMF with respect to wind speed, upwind. Note that the curves for $\sigma_0 - 10dB$ are plotted for the cases of $\theta_i = 40°$. (a) *vv* polarization (b) *hh* polarization.

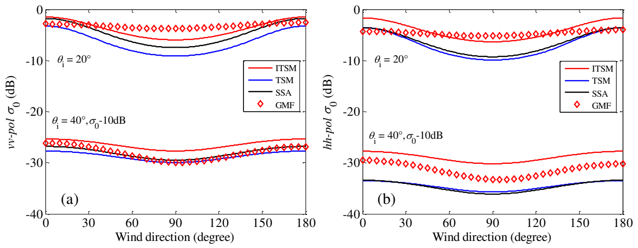

Fig. 4 The simulated results using the ITSM, the TSM and the SSA-1 are compared with those obtained using the GMF with respect to wind direction, $U_{10} = 7 m/s$, upwind. Note that the curves for $\sigma_0 - 10dB$ are plotted for the cases of $\theta_i = 40°$. (a) *vv* polarization (b) *hh* polarization.

Fig. 2 ~ Fig. 4 shows the comparisons among different models. In Fig. 2(a), Fig. 3(a), and Fig. 4(a), it can be seen that the differences among the ITSM, the TSM, the SSA-1 and the GMF are not remarkable, which implies that the impact of quasi specular scattering from stationary points is not remarkable for *vv* polarization. In Fig. 2(b), Fig. 3(b), and Fig. 4(b), for small incidence angles (about smaller than 15°), the differences among the ITSM, the TSM and the SSA-1 are not significantly. However, for moderate incidences angle, the TSM and the SSA-1 significantly underestimate the backscattering cross section for *hh* polarization, and the ITSM performs significantly better than the other two models. In fact, it remains generally unclear whether the differences between theoretical calculations and experimental data should be attributed to deficiencies of the scattering model or to the inaccurate description of sea roughness. Therefore, the inaccuracy of ITSM in crosswind direction may be caused by the inaccurate of sea spectrum.

4. CONCLUSIONS AND PERSPECTIVES

In the framework of the traditional two-scale model, this paper introduces an improved version of TSM. In the improved version, the specular scattering component is simulated using the KA-SP which does not involve the large approximation rather than the commonly used KA-GO. According to the numerical simulations, it is found that the commonly used KA-GO underestimates the scattering coefficient related to specular scattering. The simulated results using the ITSM are compared with those obtained by the TSM, the SSA-1 and the C band GMF, the comparisons indicate that the results of ITSM agree better with GMF, especially for *hh* polarization. A practical implication of this work is its potential as a method to increase the accuracy of wind-speed retrieval from scatterometric measurements. However, in this paper, only the cases for co-polarizations are considered and discussed in detail. In further work, we hope to conduct more studies on cross-polarization.

5. ACKNOWLEDGEMENTS

This work was supported in part by the Joint Funds of the National Natural Science Foundation of China (Grant No. U1906217) and the Fundamental Research Funds for the Central Universities (Grant No. 20CX06043A).

6. REFERENCES

[1] F. Ulaby, R. Moore, and A. Fung, Microwave Remote Sensing Active and Passive-Volume II: Radar Remote Sensing and Surface Scattering and Emission Theory, Artech House, Norwood, UK, 1982.
[2] H. Hersbach, CMOD5. N: A C-band geophysical model function for equivalent neutral wind. European Centre for Medium-Range Weather Forecasts, 2008.
[3] T. Elfouhaily, B. Chapron, K. Katsaros, and D. Vandemark, "A unified directional spectrum for long and short wind-driven waves," *J. Geophys. Res. Oceans*, vol. 102, no. C7, pp. 15781-15796, 1997.
[4] A. Voronovich, "Small-slope approximation for electromagnetic wave scattering at a rough interface of two dielectric half-spaces," *Waves Random Media*, vol. 4, no. 3, pp. 337-368, 1994.
[5] G. Liu et al., "A systematic comparison of the effect of polarization ratio models on sea surface wind retrieval from C-band synthetic aperture radar," *IEEE J. Sel. Top. Appl. Earth Observ. Remote Sens*, vol. 6, no. 3, pp. 1100-1108, 2013.